

Preliminary Simulation for a Slug Flow Boiling on Downward heated surface

Iljin Kim^a, Hyunwoong Lee^a, Hyungdae Kim^{a*}

^aDepartment of Nuclear Engineering, Kyung Hee University, Yongin-si, Republic of Korea

*Corresponding author: hdkims@khu.ac.kr

1. Introduction

Ex-vessel cooling strategies such as IVR-ERVC and Core-catcher has been presented in an effective way to maintain the integrity of reactor vessel during severe accident [1]. The numerous of research on safety evaluation of ex-vessel cooling strategies is continuously conducted from APR-1400 [2] to SMART [3]. Under ex-vessel cooling strategies condition, slug bubbles with high void fraction can be easily generated due to low pressure of fluid and high wall superheat. The liquid film is formed beneath the slug bubbles and the heat conduction with high heat flux occurs due to this thin layer [4]. However, the wall boiling model of Kurul and Podowski [5] generally used in most CFD software does not properly simulate the heat transfer mechanism associated with liquid film underneath slug bubbles. To perform physics-based safety evaluation of PECCS, it is necessary to track the position of slug bubbles and apply the wall boiling model considering the heat transfer through the liquid film.

In this study, a hybrid simulation methodology for flow boiling with discrete bubbles and slug bubbles on downward heated surfaces such as ERVC and core-catcher was developed and a preliminary simulation was conducted. The hybrid multiphase solver was used to selectively apply two-fluid model and VOF method to dispersed phase (discrete bubbles) and continuous fluid phase (slug bubbles), respectively. The wall heat flux partitioning model (WHFP) was developed to apply the appropriate heat transfer mechanisms to each of the dispersed and slug bubbles. The qualitative analysis with conventional CFD method was performed to evaluate the effect of the developed model on heat transfer. The qualitative analysis for distribution of void fraction was performed to evaluate the developed methodology.

2. Simulation Methods and Results

2.1 Interface capturing method

The interface tracking method of hybrid multiphase solver uses the interface compression scheme proposed by Weller [6]. This scheme solves the equation with the additional artificial compression term to the volume fraction transport equation of the multi-fluid model as shown in Eq. 1.

$$\frac{\partial \alpha_k}{\partial t} + \vec{u}_k \cdot \nabla \alpha_k + \nabla \cdot (\vec{u}_c \alpha_k (1 - \alpha_k)) = \frac{\Gamma_{ki} - \Gamma_{ik}}{\rho_k} \quad (1)$$

$$\vec{u}_c = C_{\alpha,ki} |\vec{u}| \frac{\nabla}{|\nabla \alpha|} \quad (2)$$

Here, $\alpha_k(1 - \alpha_k)$ allows the interface tracking method to work only at the interfaces. \vec{u}_c is the speed applied to the normal direction to the interface to compress volume fraction. $C_{\alpha,ki}$ is a constant for determining whether to use an interface compression method. The interface compression is enabled when $C_{\alpha,ki} = 1$, and disabled when $C_{\alpha,ki} = 0$. In addition, the constant can be set individually for each phase. Since the interface tracking method is applied only at the interface of slug bubbles, the constant is set to 0 for dispersed gas-continuous liquid interface and 1 for continuous gas-continuous liquid.

2.2 Wall heat flux partitioning model (WHFP)

● WHFP model for dispersed phase bubbles

The most popular wall heat flux partitioning model is the PRI model of Kurul and Podowski as given in Eq. 3 [5]. The model consists of single-phase convection (Eq. 4), quenching (Eq. 5), and evaporation (Eq. 6) heat transfer modes. These heat transfer mechanisms have been proposed for nucleate boiling with discrete bubbles.

$$q''_{\text{RPI}} = q''_c + q''_q + q''_e \quad (3)$$

$$q''_c = h_c A_{1\phi} (T_w - T_l) \quad (4)$$

$$q''_e = N_a \left(\frac{\pi}{6} D_{dep}^3 \right) f \rho_g h_{fg} \quad (5)$$

$$q''_q = h_q A_{2\phi} (T_w - T_l) \quad (6)$$

● WHFP model for continuous phase bubbles

Liquid film beneath a slug bubble is very thin. Conduction heat transfer across the liquid film occurs in the normal direction of the heated wall, as shown in Eq. 7. In this study, evaporation of the liquid film was not considered and its thickness was assumed constant.

$$q''_{\text{slug}} = \frac{k_l}{\delta_{film}} (T_w - T_{sat}) \quad (7)$$

● Hybrid wall boiling model

To simulate the coexistence of dispersed bubbles and slug bubbles, the contribution of the WHFP model of Eq. 3 and 7 should be appropriately combined. The contribution of each WHFP model at a position was determined by a weighting function correlated with void fraction of slug bubbles (α_{slug}), as shown in Eq. 8. The upper-lower limit of the volume fraction of slug bubbles to be applied to the weighting function was set as $\alpha_2^f = 1.0$ and $\alpha_1^f = 0.5$, referring to the values in [7].

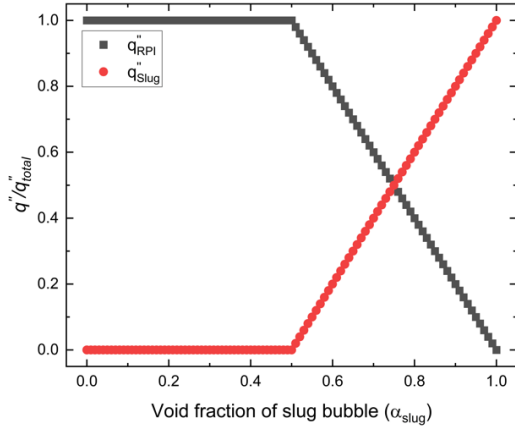


Fig. 1. Heat flux ratio according to the void fraction of slug bubble

Table I: Major conditions of slug flow boiling simulation

Variable	Value
Pressure	120 kPa
Subcooling	1.2 K
Mass flux	300 kg/m ² s
Heat flux	100 ~ 300 kW/m ²

Table II: Mesh information for the sensitivity test

Mesh size	Coarse	Medium	Fine
Number of meshes	75 × 10	150 × 20	225 × 30
Number of mesh/m	500	1000	1500

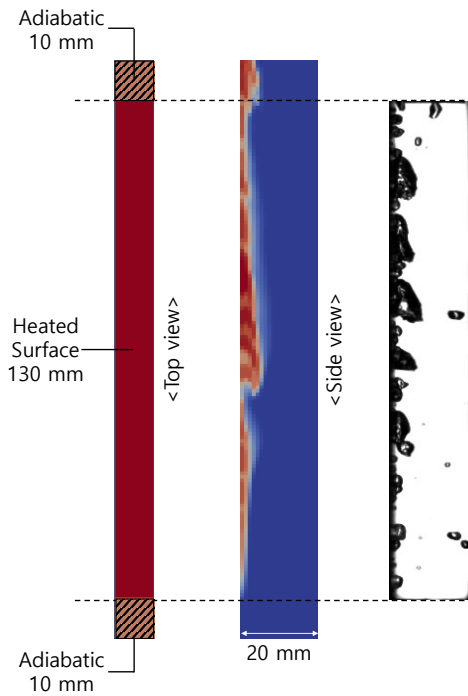


Fig. 2. Two-dimensional simulation domain.

The WHFP model for slug flow boiling using the weighting function is shown in Eq. 9, and the contribution of WHFP model according to the volume fraction of slug bubbles is shown in Fig. 1.

- Blending function for WHFP model

$$H(\alpha_{slug}) = \max\left(0, \min\left(1, \frac{\alpha_2^f - \alpha_{slug}}{\alpha_2^f - \alpha_1^f}\right)\right) \quad (8)$$

- WHFP model for all bubbles

$$q''_w = [1 - H(\alpha_{slug})]q''_{RPI} + H(\alpha_{slug})q''_{slug} \quad (9)$$

2.3 Wall boiling closure models

The RPI WHFP model was developed in consideration of the heat transfer mechanisms of nucleate boiling as described above. To use the RPI model, closure models for nucleation site density, bubble departure diameter, and bubble departure frequency are needed. The commonly used closure models in OpenFOAM releases were used as below.

- Nucleation site density: Lemmert-Chawla [8]

$$N_a = C_n N_{a,Ref} \left(\frac{T_w - T_{sat}}{\Delta T_{Ref}}\right)^n \quad (10)$$

- Bubble departure frequency: Cole [9]

$$f = \sqrt{\frac{4g(\rho_l - \rho_g)}{3D_{dep}\rho_l}} \quad (11)$$

- Bubble departure diameter: Kocamustafaogullari-Ishii [10]

$$D_{dep} = 2.5 \times 10^{-5} \left(\frac{\rho_l - \rho_g}{\rho_g}\right)^{0.9} \theta \sqrt{\frac{\sigma}{g(\rho_l - \rho_g)}} \quad (12)$$

2.4 Initial and boundary conditions

The slug flow boiling simulation was conducted in the subcooled condition as seen Fig. 2. The heated surface of 130 mm on the top side of simulation domain. Two adiabatic areas of 10 mm exist in the channel entrance and exit regions. The major condition of simulation is summarized in table 1. The fluid pressure is 120 kPa, and the subcooling and velocity of liquid are 1.2K and 300 kg/m²s respectively. The results of simulation were compared with the applied heat flux changed to 100 ~ 300 kW/m².

2.5 Mesh sensitivity test

The mesh sensitivity test was performed to achieve mesh-independent result of the slug bubbles' interface. The mesh configuration used for dependency analysis is that the square mesh is uniformly distributed in the simulation domain. The size of square mesh was set to 3 different sizes as shown in table 2.

As a result of the analysis (Fig. 3), in the case with the coarse mesh, the shape of bubbles was like film boiling rather than slug bubbles. As the mesh size increased, the thickness of the interface was thinned. In addition, as the size of the mesh decreased, the shape of the bubbles tends to be deformed by the drag at the interface caused by the relative velocity of the bubbles and liquids. As a result of mesh sensitivity test, the simulation using the fine mesh size was performed.

2.5 Simulation results

As shown in Fig. 4, slug flow boiling simulation was performed on a downward-facing heated surface with an inclined angle of 10° , and major simulation conditions are listed in Table 2.

At the low heat flux condition, the nucleate bubbles were generated on the heater surface. The bubbles grew or merged with other bubbles as it moved along the heated surface. In the case of 200 kW/m^2 , the generation and merging of bubbles increased, and it was confirmed that bubbles similar to slug bubbles were formed at the exit of the simulation domain. At the highest heat flux, 300 kW/m^2 , the nucleate bubbles generated on the overall heating surface merged to form slug bubble. The slug bubble swept through the entire heated surface, and the process of transition the slug bubbles again by the formation and merger of the nucleate bubbles was well simulated.

3. Conclusions

The methodology for the slug flow boiling simulation on the downward heated surface was developed, and a preliminary simulation was conducted. Using hybrid multiphase solver, the two-fluid model was applied to nucleate bubbles, and the VOF interface tracking method was applied to slug bubbles. To simulate the dispersed and slug bubbles simultaneously, the WHFP model was developed that reflects the contribution of each heat transfer mechanisms. The preliminary simulation was performed on the downward heated surface according to the change of heat flux for qualitative evaluation, and the slug bubble formation by bubble merging was well simulated. In future studies, the shape of slug bubble and contribution of heat transfer mechanisms will be validated using flow boiling experimental data on a downward-facing wall.

ACKNOWLEDGEMENT

This study was sponsored by the Ministry of Science and ICT and was supported by Nuclear Research & Development program grant funded by the National Research Foundation (NRF) (Grant code: 2017M2A8A4015283).

$G = 300 \text{ kg/m}^2\text{s}, q_w'' = 300 \text{ kW/m}^2\text{s}, 90^\circ$ (vertical flow)

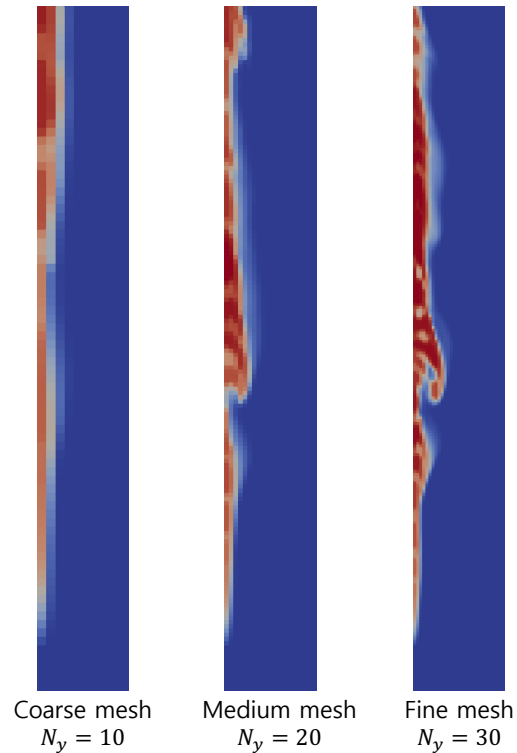


Fig. 3. Results of mesh sensitivity test.

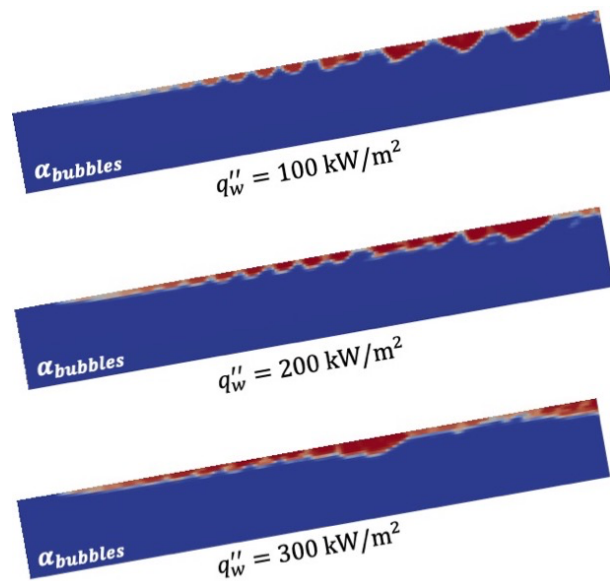


Fig. 4. Distribution of void fraction with different heat fluxes.

REFERENCES

- [1] R. E. Henry and H. K. Fauske, "External cooling of a reactor vessel under accident conditions," 1993.
- [2] K. S. Ha, F. B. Cheung, R. J. Park, and S. B. Kim, "Evaluations of two-phase natural circulation flow induced in the reactor vessel annular gap under ERVC conditions," *Nuclear Engineering and Design*, vol. 253, pp. 114–124, 2012, doi: 10.1016/j.nucengdes.2012.08.004.

- [3] R. J. Park, D. Son, H. S. Kang, S. M. An, and K. S. Ha, "Development of IVR-ERVC evaluation method and its application to the SMART," *Annals of Nuclear Energy*, 2021, doi: 10.1016/j.anucene.2021.108463.
- [4] H. T. Kim and K. H. Bang, "An experimental study of flow boiling from downward-facing heated wall in inclined channels," *International Journal of Heat and Mass Transfer*, vol. 133, pp. 920–929, 2019, doi: 10.1016/j.ijheatmasstransfer.2018.12.183.
- [5] N. Kurul and M. Z. Podowski, "MULTIDIMENSIONAL EFFECTS IN FORCED CONVECTION SUBCOOLED BOILING," in *Proceeding of International Heat Transfer Conference 9*, 1990, pp. 21–26. doi: 10.1615/IHTC9.40.
- [6] K. E. Wardle and H. G. Weller, "Hybrid multiphase CFD solver for coupled dispersed/segregated flows in liquid-liquid extraction," 2, vol. 2013, no. 1, 2013, doi: <https://doi.org/10.1155/2013/128936>.
- [7] A. Ioilev *et al.*, "Advances in the modeling of cladding heat transfer and critical heat flux in boiling water reactor fuel assemblies," *Proceedings - 12th International Topical Meeting on Nuclear Reactor Thermal Hydraulics, NURETH-12*, 2007.
- [8] LEMMERT M. and CHAWLA J. M., *INFLUENCE OF FLOW VELOCITY ON SURFACE BOILING HEAT TRANSFERT COEFFICIENT*. 1977, pp. 231–247.
- [9] R. Cole, "A Photographic Study of Pool Boiling in the Region of the Critical Heat Flux."
- [10] G. Kocamustafaogullari and M. Ishii, "Aire interfaciale et densite de sites de nucleation dans les systemes en ebullition," *International Journal of Heat and Mass Transfer*, vol. 26, no. 9, pp. 1377–1387, 1983, doi: 10.1016/S0017-9310(83)80069-6.